Relation between interfacial magnetism and spin-dependent scattering at non-ideal Fe/Cr and Fe/V interfaces

R. Coehoorn

Philips Research Laboratories, Prof. Holstlaan 4, 5656 AA Eindhoven, The Netherlands

Abstract

First principles band structure calculations have been performed for (110) and (100) Fe/Cr and Fe/V superlattices with mixed monolayers at the interfaces, with atomic concentrations in the mixed layers throughout the entire concentration range. In addition, (211) and (111) superlattices with perfect interfaces have been studied. For Fe/V systems the moments at the interfaces depend strongly on the nearest neighbour environment. Conversely, Fe and Cr moments at Fe/Cr interfaces show almost no dependence on the nearest neighbour environment. We explain the latter behaviour as the result of competing antiferromagnetic exchange interactions at the interface, and discuss why this behaviour is crucial to the strong spin dependence of scattering at Fe/Cr interfaces, which gives rise to the very large giant magnetoresistance effect observed for Fe/Cr multilayers. Implications are given for the temperature dependence of the GMR ratio.

1. Introduction

The giant magnetoresistance (GMR) effect in magnetic multilayers originates from spin-dependent scattering in the bulk of the magnetic layers, and at the interfaces. In order to disentangle these two possible contributions experimental studies of the layer thickness dependences of the GMR effect have been set up for various multilayer systems, using the Current In Plane (CIP) [1–3] as well as the Current Perpendicular to the Planes (CPP) geometry [4]. It has become clear that spin-dependent scattering at the interfaces contributes significantly to the GMR effect in e.g. Co/Cu and Co/Ag systems [4,5], and in Fe/Cr systems [3], although there is an additional spin-dependence of scattering in the bulk of the layers [2–4]. From the work by Gijs et al., e.g., it follows that the spin-asymmetry ratio for scattering within bulk Fe or Co, $\alpha_{bulk} \equiv \rho_{\downarrow}/\rho_{\uparrow}$, equals about 0.4 and 2.5, respectively, whereas the spin asymme-

try ratios for scattering at Fe/Cr and Co/Cu interfaces equal about 0.1 and 20. The MR ratio of Fe/Cr systems may be increased by decreasing the Fe layer thickness, as has been demonstrated by Schad et al. [6]. For Fe/Cr superlattices with Fe layer thicknesses of only 4.5 Å they obtained an MR ratio of 220% at 1.5 K. This is the highest GMR ratio for metallic multilayers reported so far, and shows that spin-dependent scattering at the Fe/Cr interfaces is by itself sufficient for obtaining a very large GMR effect.

In spite of this progress in the understanding of the importance of the contribution of spin-dependent diffusive scattering at the interfaces, we are just beginning to understand how this scattering might depend on the interface structure and magnetism. Diffusive scattering arises as a consequence of lateral variations in the atomic potentials, resulting from imperfections. Theoretical studies of interface scattering should therefore start with a certain model

for the interface structure, and should take into account that the effective potentials of atoms in the interface region may be modified with respect to the atomic potential in the bulk metals due to the interaction with neighbour atoms of a different type. In our point of view, in metallic systems the largest modification on the effective atomic potentials is due to the change of magnetic moments, with respect to the bulk value; charge transfer effects are usually very small.

The purpose of this paper is to present a more quantitative discussion of these ideas, as applied to spin dependent scattering at Fe/Cr and Fe/V interfaces. Our model of the interface is that of a mixed layer with monolayer (ML) thickness. Such interfaces have been realized by MBE growth, as follows by the observation of 2 ML oscillations in the interlayer exchange coupling [7], and from the analysis of Mössbauer spectra [8]. Recently Beliën et al. have demonstrated that limiting roughness to a monolayer, leading to a moderate step density, and avoiding interdiffusion, is important for obtaining an optimized GMR ratio for Fe/Cr superlattices [9].

We first present results of a study by means of first principles band structure calculations of the relation between the interface structure and magnetism. We have carried out supercell calculations for (110) and (100) oriented Fe/Cr multilayers with ordered mixed monolayers at the interfaces. The Fe concentration x_{Fe} in the mixed monolayer is varied throughout the entire concentration range. It should be noted that our calculations are an extension of the work performed by Itoh et al. [10] on 'interface impurities' (the limiting cases $x_{Fe} \to 0$ and $x_{Fe} \to 1$). In analogy to bulk alloys, one may view the systems studied as ordered approximations to 'monolayer interface alloys'. Similar questions as in the case of bulk alloy systems, such as on the change of magnetic moments upon 3-D ordering, may also be raised in the case of these quasi 2-D systems. This issue will be discussed briefly.

The main result is that the magnetic moments of Fe and Cr atoms in such one monolayer thick mixed interface layers only very weakly depend on the concentration of Fe and Cr within the mixed layer, and on the specific type of ordering: Fe moments are equal to $1.95 \pm 0.1 \mu_B$ and Cr moments vary between -0.2 and $-0.5 \mu_B$. As far as the Cr moments

are concerned, this is, on first sight, a very surprising result: Cr impurities in an Fe matrix show a much larger induced magnetic moment. The calculated moment is $-1.71 \mu_B$ [11], which falls in the range of values observed experimentally [12]. In order to elucidate the underlying mechanism we have carried out additional studies for the perfect, but more open, Fe/Cr (211) and (111) interfaces, and for perfect and non-ideal Fe/V interfaces. In contrast to the case of Fe/Cr interfaces, Fe/V systems are shown to behave as expected: induced V moments at interfaces increase monotonically with the number of Fe nearest neighbours, extrapolating to the value of about $-1.2 \mu_B$ per V atom for a V impurity in an Fe matrix. We will argue that the crucial difference between the two systems is the antiferromagnetic interatomic exchange between successive Cr layers, which is absent in the case of V. This leads to small Cr moments due to competing antiferromagnetic exchange interactions. We point out that a similar mechanism is operative in Fe–Cr bulk alloys. Dreyssé et al. have recently presented similar ideas for the case of Fe/Cr stepped interfaces [13].

Finally, we will discuss the relationship between spin-dependent scattering and interface magnetism, using an approach which we proposed earlier [11]. We will argue that the small, concentration independent value of the Cr moments in mixed interfaces layers is crucial to the strong spin-dependent scattering at the interface.

Part of the results presented in this paper have already been briefly discussed in an earlier publication [14].

2. Structural details

From a series of trial calculations we have found that it is entirely adequate, when focussing at the magnetism of magnetic moments in mixed monolayer interface layers, to perform all calculations for (110) and (100) superlattices of the type:

$$5 \, ML \, Fe / 1 \, ML \, Fe_x Cr_{1-x} / 5 \, ML \, Cr / 1 \, ML \, Fe_x Cr_{1-x},$$

and similarly for Fe/V systems. We have carried out our calculations for $x = 1$ (perfect interfaces), $x = 3/4$, $1/2$ and $1/4$, and in some cases for $x = 1/8$.
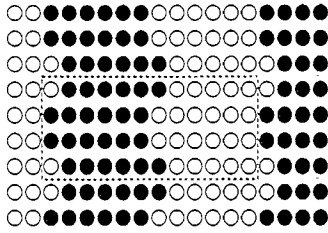
Fig. 1. Schematic cross-section of a superlattice with ordered mixed interface layers, and layer thicknesses as discussed in this paper. The dashed box indicates the size of the supercell.

A schematic picture of the systems studied is shown in Fig. 1.

Fig. 2 shows the structure of the mixed monolayers for (100) and (110) systems. For Fe/V (100) systems with $x = 1/2$ two mixed layer configurations, indicated with I and II, were considered. For (110) systems with $x = 1/4$ and $3/4$ only the configurations I were considered. A comparison with the results for laterally doubled cells with configuration II, for which the shortest distance between minority-type atoms in the mixed monolayer is about 22% larger, would be of interest in future studies. The calculations for (211) and (111) oriented layers with perfect interfaces have been carried out for 8 ML Fe
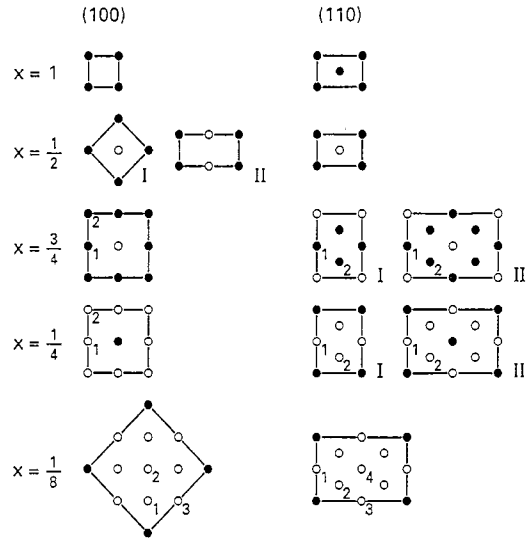

Fig. 2. 2-Dimensional unit cells within the mixed interface layers. Filled and open circles denote Fe and Cr(V) atoms. The numbering of the atoms corresponds to the order in which the local environment and the moments are given in Tables 2 and 3.

/10 ML (Cr,V) and 10 ML Fe/14 ML (Cr,V) systems, respectively.

In the case of Fe/Cr systems all atoms are assumed to be situated on the lattice sites of a body

Table 1
Structural data of basic cells from which unit cells of bcc-based superlattices with various orientations, and with perfect interfaces may be constructed (see text). All lengths are expressed in the cubic lattice parameter a of the underlying bcc lattice.

	Cell symmetry	Cell dimensions	Interplanar distance	In-plane nearest neighbour distance	Atomic positions
(110)	ortho-rhombic	$a' = a$ $b' = \sqrt{2}\,a$ $c' = \sqrt{2}\,a$	$\frac{1}{2}\sqrt{2}\,a$	$\frac{1}{2}\sqrt{3}\,a$	$(0,0,0),(\frac{1}{2},\frac{1}{2},0)$ $(\frac{1}{2},0,\frac{1}{2}),(0,\frac{1}{2},\frac{1}{2})$
(100)	cubic	$a' = a$ $b' = a$ $c' = a$	$\frac{1}{2}a$	a	$(0,0,0),(\frac{1}{2},\frac{1}{2},\frac{1}{2})$
(211)	ortho-rhombic	$a' = \frac{1}{2}\sqrt{3}\,a$ $b' = \sqrt{2}\,a$ $c' = \sqrt{6}\,a$	$\frac{1}{6}\sqrt{6}\,a$	$\frac{1}{2}\sqrt{3}\,a$	$(0,0,0),(\frac{1}{3},\frac{1}{2},\frac{1}{6})$ $(\frac{2}{3},0,\frac{1}{3}),(0,\frac{1}{2},\frac{1}{2})$ $(\frac{1}{3},0,\frac{2}{3}),(\frac{2}{3},\frac{1}{2},\frac{5}{6})$
(111)	hexa-gonal	$a' = \sqrt{2}\,a$ $b' = \sqrt{2}\,a$ $c' = \frac{1}{2}\sqrt{3}\,a$	$\frac{1}{6}\sqrt{3}\,a$	$\sqrt{2}\,a$	$(0,0,0),(\frac{2}{3},\frac{1}{3},\frac{1}{3})$ $(\frac{1}{3},\frac{2}{3},\frac{2}{3})$

centered cubic lattice, with the cubic lattice parameter of α-Fe: $a = 2.867$ Å. The atomic positions can most easily be found by considering that the unit cell of the superlattice can be viewed as a stacking in the c-axis direction of an integral number of basic cells (if no distinction between chemically different atoms is made). Their thicknesses are 2, 2, 6 and 3 atomic planes for the (110), (100), (211) and (111) systems, respectively, and in the case of perfect interfaces they have orthorhombic, cubic, orthorhombic and hexagonal shapes, respectively. In Table 1 we give the cell dimensions and the interplanar distances, the distance between nearest neighbours within an atomic plane perpendicular to the c-axis, and the atomic positions.

In the case of Fe/V systems the 5.6% lattice mismatch between Fe and V is taken into account by a compression of the V and mixed layers in the lateral directions, in order to form a coherent superlattice with the undeformed Fe sublattice, and an expansion in the perpendicular direction, in order to keep the local atomic volumes unchanged. This implies that the distances between the V layers are 11% larger than in elemental V, that at perfect interfaces the distance between Fe and V layers is equal to the average of the interlayer distances of elemental Fe and V, and that the distances between the mixed layers and the Fe and V layers vary according to the concentration of the mixed layers. Possible buckling effects have been neglected: within each layer the atoms have the same c-axis coordinate, irrespective of their chemical nature and symmetry type.

Table 2 gives for all atoms in the systems considered the total number of nearest and next nearest neighbours which are chemically different from the central atom. Note that for atoms on a bcc lattice the total number of nearest and next nearest neighbours is 14.

3. Calculational method

First principles self-consistent band structure calculations were performed using the Augmented Spherical Wave (ASW) method [15]. Exchange and correlation were treated within the local spin density formalism [16], using the parameter values given by Janak [17]. Within the ASW method the atomic spheres approximation (ASA) is made: the potential within a spherical region, centered around the atomic sites, is spherically symmetric. The radii, r_{WS}, of the Wigner–Seitz spheres at Fe and Cr sites were taken to be identical to the sphere radius for bcc Fe at the experimental lattice constant: $r_{WS} = 1.411$ Å. For V atoms we used $r_{WS} = 1.490$ Å, corresponding to the sphere radius for elemental V at the experimental lattice constant. The calculations are scalar relativistic, i.e. mass-velocity and Darwin terms are included, but spin–orbit interaction is neglected. The set of basis functions included 4s, 4p and 3d states, whereas 4f contributions where included in the internal summation of the three center contributions to the matrix elements. This can be viewed as treating 4f states as a perturbation.

In order to efficiently scan the Brillouin zone (BZ) we took advantage of the large size of the unit cell in the z-direction, perpendicular to the layers, by restricting the grid in the k_z-direction to only one point. Calculations for perfect interfaces with more

Table 2

Numbers of nearest and next nearest neighbours which are chemically different, for Fe and Cr or V atoms in mixed interface layers with Fe concentration x_{Fe}. The ordering which corresponds to each concentration is shown in Fig. 1. In the case of chemically similar but crystallographically different atoms, the numbers of chemically different neighbours are given in the order indicated by the numbering in Fig. 1. The cases $x_{Fe} = 1$ and $x_{Fe} = 0$ correspond to perfect interfaces.

System	x_{FE}	Fe	Cr,V
(110)	1	4	–
	3/4	6,6	10
	1/2	8	8
	1/4	10	6,6
	1/8	10	6,5,4,4
	0	–	4
(100)	1	5	–
	3/4	7,5	9
	1/2 (I)	9	9
	1/2 (II)	7	7
	1/4	9	7,5
	1/8	9	6,5,5
	0	–	5
(211)	1	6	–
	0	–	6
(111)	1	7	–
	0	–	7

points along the k_z-direction confirmed the appropriateness of this procedure. The number of k-points in the irreducible part of the BZ varied from 42 and 32 for $x = 1$ to 3 and 4 for $x = 1/8$, for (100) and (110) systems, respectively. The numerical accuracy of the converged magnetic moments is $0.03 \mu_B$ per Fe atom for the largest cell, and better for the smaller cells.

4. Results

4.1. Perfect interfaces

In Fig. 3a,b the calculated magnetic moments of Fe/Cr and Fe/V superlattices with perfect interfaces are shown. Numerical values of the magnetic moments of the atoms at the interfaces are contained in Table 3. General features of the perfect superlattices are (i) that the calculated Fe moments at the interfaces are a few tenths of μ_B lower than the calculated bulk value $(2.26 \mu_B)$, (ii) that the Cr layers show an oscillatory magnetization, and (iii) that in the V layers a magnetic polarisation is induced whose amplitude decreases rapidly towards the center of the layers. The Fe moments in Fe/Cr systems are in all cases larger than on the corresponding planes in Fe/V systems. We checked that the Fe and Cr (or V) moments in the first and second layer from the interface are not significantly different from the Fe and Cr (or V) moments calculated for systems with thicker Fe and Cr (or V) layers. In the case of Fe/Cr (100) or (110) systems, the observed 2 ML oscillation of the Cr moment is, of course, frustrated in the case of an even number of Cr layers, However, this does not affect the calculated moments at the interfaces. For a 6 ML Fe/ 8 ML Cr (100) superlattice, e.g., we found that the absolute value of the Cr moments in the first, second, third and fourth layer from the mixed layer are 0.00, 0.04, 0.04 and $0.21 \mu_B$

Fig. 3. Magnetic moments in (a) Fe/Cr and (b) Fe/V superlattices with perfect interfaces, for various orientations. For clarity, data for Fe/Cr (100), (211) and (111) have been shifted by -0.6, -1.4 and $-2.0 \mu_B$, respectively. Data for Fe/V (100), (211) and (111) have been shifted by -0.6, -1.2 and $-1.8 \mu_B$, respectively.
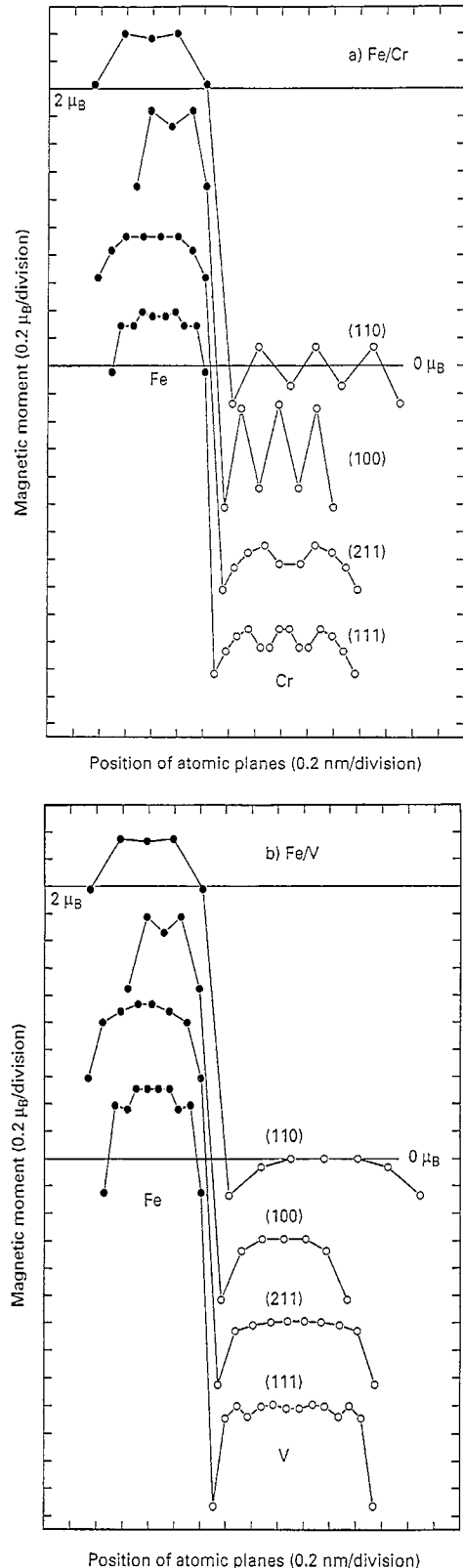
smaller than for the 5 ML Fe/7 ML Cr (100) superlattices for which the moments are shown in Fig. 3a. Apparently, the effect of the frustration in the moment is highly localized in the center of the Cr layer.

In the series of (110), (100), (211) and (111) superlattices with perfect interfaces the number of chemically different neighbours of an atom at the interface increases from 4 to 7 (see Table 1). In the case of Fe/V systems this leads to a gradual decrease of the Fe moment at the interfaces, and a gradual increase of the induced V moments at the interfaces. However, for the same series of Fe/Cr superlattices such a trend is not found: the Fe moments at the interface are lower than the bulk value, but almost independent of the number of Cr neighbours, and the Cr moments at the interface do not increase with the number of Fe nearest neighbours, but are maximal for (100) superlattices.

4.2. Imperfect interfaces

Fig. 4 shows the calculated Fe, Cr and V magnetic moments in the one monolayer thick ordered mixed interface layers for (100) and (110) Fe/Cr and Fe/V superlattices, as a function of the concentration of Fe atoms in the mixed layer. In the limiting cases $x = 1$ and $x = 0$ the figure gives, of course, the Fe and Cr (or V) moments, respectively, at the perfect interfaces. The figure shows that Fe moments in the mixed layers decrease strongly with decreasing Fe concentration in the case of Fe/V systems, whereas such a decrease is absent or very small for Fe/Cr systems. Similarly, the absolute value of the V moments decreases strongly with decreasing Fe concentration, whereas the Cr moments in the mixed layer are quite stable, in particular for (100) systems. The magnetic moments of V interface impurities for (110) and (100) systems is estimated by extrapola-

Table 3

Calculated magnetic moments in one ML thick interface layers. The chemical ordering which corresponds to the concentration x_{Fe} of Fe atoms has been shown in Fig. 1. No calculations have been performed for Fe/Cr systems with $x = 1/8$. Units: μ_B.

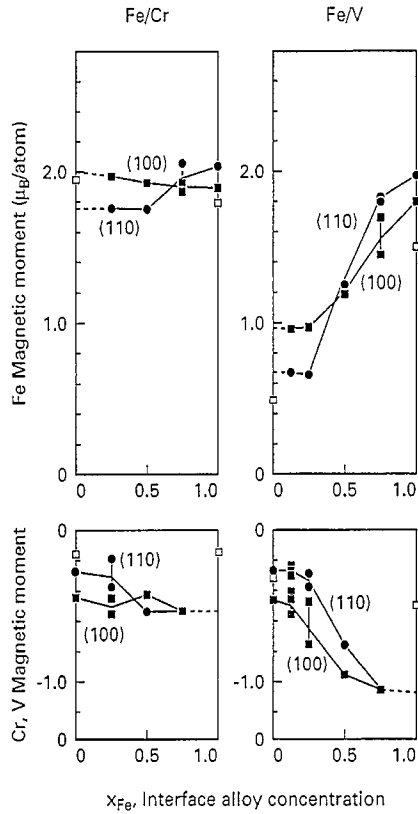|	x_{Fe}	Fe/Cr		Fe/V	
		Fe	Cr	Fe	V
(110)	1	2.04	–	1.99	–
	3/4	2.09/1.90	–0.55	1.82/1.78	–1.06
	1/2	1.77	–0.55	1.26	–0.75
	1/4	1.79	–0.18/–0.35	0.67	–0.30/–0.37
	1/8			0.69	–0.30/–0.32/ –0.27/–0.22
	0	–	–0.27	–	–0.27
(100)	1	1.90	–	1.85	–
	3/4	1.92/1.88	–0.52	1.45/1.71	–1.06
	1/2 (I)	1.95	–0.41	1.19	–0.94
	1/2 (II)	1.90	–0.53	1.46	–0.74
	1/4	1.98	–0.45/–0.55	0.97	–0.76/–0.49
	1/8			1.04	–0.66/–0.53/ –0.50
	0	–	–0.42	–	–0.43
(211)	1	2.04	–	1.80	–
	0	–	–0.21	–	–0.43
(111)	1	1.97	–	1.55	–
	0	–	–0.23	–	–0.72

Fig. 4. Dependence of calculated magnetic moments in the mixed interface layers on the Fe concentration within this layer, for (110) (circles) and (100) (squares) Fe/Cr and Fe/V superlattices. Full lines connect the weighted averaged moments. For (100) systems with $x_{Fe} = 1/2$ data for configuration I are given. Broken lines give the extrapolation to interface impurities. Calculated moments for atoms at perfect interfaces and for interface impurities, as obtained by Itoh et al. [10] are given by open signs.
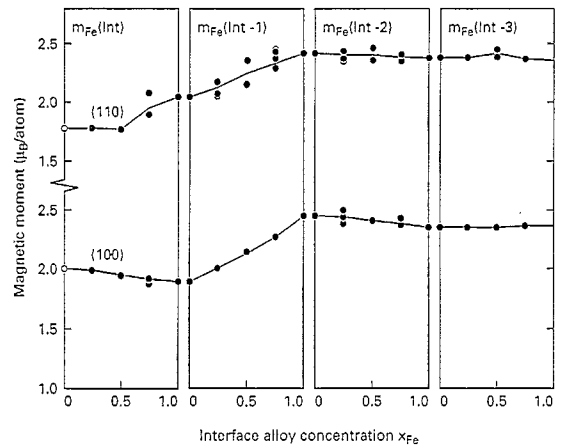

Fig. 5. Dependence on the Fe concentration of the mixed interface layer of calculated Fe magnetic moments in all layers of the system, for (110) and (100) Fe/Cr superlattices. Open circles represent the values of interface impurities, as obtained by extrapolation.

tion to be about $-1.1\mu_B$, which is about twice the moment estimated for Cr interface impurities. The physical origin of this remarkable result, and the consequences for spin dependent interface scattering, are discussed in Section 5.

Figs. 5 and 6 show for (100) and (110) Fe/Cr superlattices the Fe and Cr moments in the other layers, plotted in the same manner as in Fig. 4. One may conclude from Fig. 5 that a change of the concentration of the interface layer mainly affects the Fe moments in the layer one below the mixed layer. The moments in the second and third layer are already quite independent of the concentration in the mixed layer, although slightly above the calculated value for bulk Fe ($2.26\mu_B$). On the other hand, the

moments in the Cr layers away from the mixed layer are very sensitive to the precise concentration of the mixed layer, as may be expected from the consideration that the increase of x_{Fe} from 0 to 1 corresponds to a change of the Cr thickness from 7 to 5 ML. Within a simple model, such as proposed by Wang et al. [18] for the dependence of interlayer exchange coupling on the interface roughness, the Cr moments
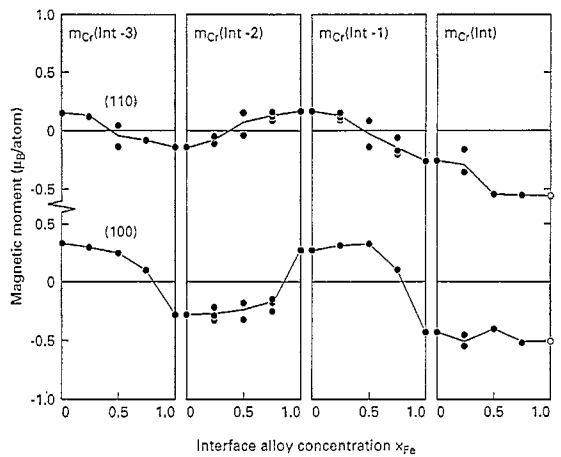

Fig. 6. Dependence on the Fe concentration of the mixed interface layer of calculated Cr magnetic moments in all layers of the system, for (110) and (100) Fe/Cr superlattices. Open circles represent the values of interface impurities, as obtained by extrapolation.

in the middle of the spacer are expected to be very close to zero for $x_{Fe} = 0.5$ due to frustrated exchange interactions. The effective Cr thickness is then 6 ML. It may be seen from Fig. 6 that this situation is found indeed for (110) systems, but that for (100) systems the crossover takes place in between $x_{Fe} = 0.75$ and $x_{Fe} = 1$. This, although indirectly, suggests that a very small degree of interface roughness might in some cases strongly affect the sign of interlayer exchange coupling.

First principles band structure calculations for Fe/Cr(100) multilayers with perfect interfaces have been performed earlier by Herman et al. [19], and for Fe/V(100) multilayers by Hamada et al. [20]. Qualitatively, our results show good agreement with this work, confirming the antiparallel coupling between Fe and Cr (or V) moments across the interface, the oscillatory magnetization within the Cr layers, and the rapid decrease of the induced V moments with increasing distance to the interfaces. Quantitative differences with respect to the size of the moments may be attributed to different structural and/or calculational details. In addition, our results show good qualitative agreement with the results from tight-binding calculations [10,21,22]. Calculated moments at perfect (100) interfaces and at interface impurities, obtained by Itoh et al. [10], are given in Fig. 4 by empty squares. There are some small but significant differences with our results, in particular with respect to the Fe moments in the Fe/V interface layers, and the moments of Cr and V interface impurities. At this point we cannot judge whether, and to what extent, this can be explained by one or more of the approximations made in [10], such as the neglect of s and p states, neglecting the intra-atomic exchange potential for Cr and V, or the neglect of lattice relaxation in the case of Fe/V.

4.3. Effective dead layer thickness

Before discussing the implications of these results to spin-dependent interface scattering, a comparison with experimental data on the magnetic moments near interfaces would be in place. To our point of view, quantitative atom resolved information on magnetic moments near interfaces may, in principle, best be derived from an analysis of observed hyperfine fields, making use of predictions of hyperfine

parameters from ab initio band structure calculations. Although detailed studies of hyperfine fields are available for Fe/Cr and Fe/V [23] systems, such a quantitative analysis is impeded by some errors in first principles calculation of hyperfine fields. Recently, we have given a critical analysis of the various contributions to the hyperfine fields for the elemental ferromagnetic metals, and have suggested a possible empirical correction procedure for a systematic error in the calculated Fermi-contact contribution to the hyperfine field [24]. In a future paper, we will make use of this correction procedure, and compare theoretical and experimental hyperfine fields.

Averaged information on interfacial magnetism may be obtained from the comparison of the calculated and experimental 'dead layer thickness'. This quantity is defined as the layer thickness which per interface should be subtracted from the thickness of a ferromagnetic layer, in order to obtain the magnetization of the total superlattice on the basis of bulk magnetic moments. Positive dead layer thicknesses may arise from decreased moments in the ferromagnetic layers near the interfaces, and/or from the antiparallel alignment of the induced moments in the spacer layer, as in the case of Fe/V. The calculated effective dead layer thickness for (110) and (100) Fe/V systems is given in Fig. 7. The magnetization is slightly more reduced in the case of (100) systems than for (110) systems, and the effective dead layer thickness reaches its maximum for $x_{Fe} = 0.5$, where it amounts to approximately 0.91 and 0.75 Å, respectively. The agreement with experimental values
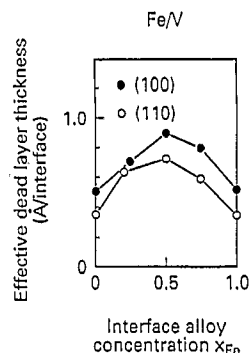
Fig. 7. Variation of the effective 'dead layer thickness' for (110) and (100) Fe/V superlattices, as a function of the concentration of Fe moments in the mixed layer at the interfaces.

(about 1.0 Å for evaporation and sputter deposited systems [25]) is good.

For Fe/Cr systems the 2 ML oscillations in Cr make the concept of a dead layer thickness less practical.

5. Discussion

5.1. Magnetic moments in mixed layers

Fig. 8 shows that the magnetic moments per Fe and Cr atom in mixed Fe/Cr interface layers, and at perfect interfaces, are only very weakly dependent on the number of Cr and Fe nearest neighbour atoms (summed over the nearest and next nearest neighbour shells). On the other hand, as shown in Fig. 9, the magnetic moment per Fe atom in mixed Fe/V interface layers, and at perfect interfaces, decreases quite significantly with an increasing number of V neighbour atoms. The calculated magnetic moment per V atom in mixed interface layers behaves quite regularly, too. It increases nearly monotonically with the number of Fe neighbours, to the value of $-1.21\mu_B$ for the moment calculated for V impurity atoms in Fe [11]. The figure shows that the differences between the Fe and V moments in interface layers of type I and type II with $x_{Fe} = 1/2$, and between the concentration dependences of Fe and V moments for (110) and (100) oriented systems, may be well understood in terms of the differences in the local environments.

It is of interest to compare our results to the average moments for random substitutional bulk alloys, as obtained from Coherent Potential Approximation (CPA) calculations. Results reported for Fe–Cr and Fe–V systems by Butler et al. [26] and by Johnson et al. [27], respectively, are indicated in Figs. 8 and 9 by dashed lines. In the limiting cases (bulk Fe, and Cr or V impurities in Fe), these results agree well with our ASW results. Qualitatively, the variations of moments upon a change of the local surroundings are quite similar for the moments in mixed interfaces layers, as compared to moments in dilute random alloys. The largest difference is observed for the variation of V moments with the number of Fe neighbours. We ascribe this to the fact that Fe neighbours of V atoms at interfaces have, on
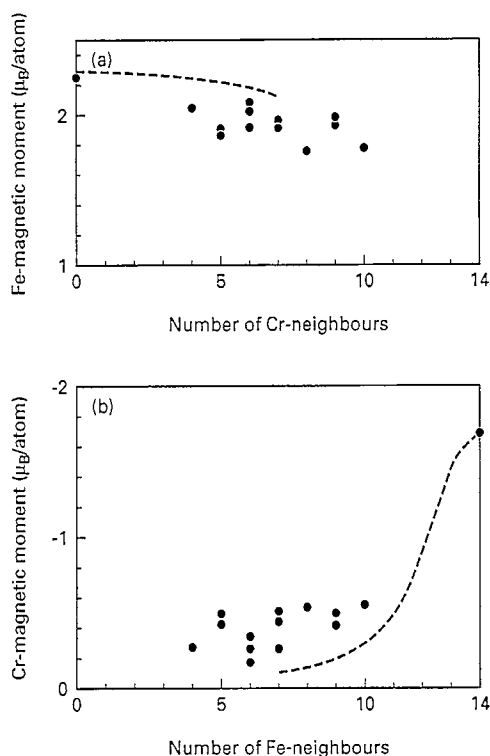

Fig. 8. Dependence of the calculated (a) Fe and (b) Cr magnetic moments, at perfect interfaces and in mixed interface layers of Fe/Cr superlattices (filled circles). The figure also includes the calculated bulk Fe moment and impurity Cr moment. The dashed lines give the average Fe and Cr moments for random substitutional bcc-type alloys, as a function of the average numbers of nearest neighbours, as calculated by Butler et al. [26].

the average, larger moments than Fe neighbours in bulk Fe–V alloys.

The Fe–Cr case is even more interesting. As shown by the calculations by Butler et al. [26], which are supported by results from neutron scattering experiments [12], Cr moments in Fe–Cr alloys increase dramatically below a Cr concentration of about 15 atomic percent. For larger Cr concentration, Cr moments are very small. Similarly, we have found that Cr moments in mixed interface layers are very small. We propose that the mechanism which gives rise to these small Cr moments is the same in both cases, viz. the competition between antiferromagnetic (AF) exchange interactions, leading to frustration. Referring to the example of a Cr interface impurity, shown in Fig. 10, the competing antiferromagnetic interactions are the AF exchange interactions between the

Cr interface impurity and the Fe neighbours, between the Fe neighbours and the Cr neighbours, and between the Cr neighbours and the interface impurity. The AF Fe–Cr exchange interaction is stronger than the AF Cr–Cr interaction. The resulting frustration may be alleviated either by a rotation of the direction of the moment of the Cr interface impurity atom, or by a decrease of its value. Calculations by Gautier et al. [28] indicate that frustration effects in Fe/Cr systems are, in the case of thin layer thicknesses, alleviated by a reduction of the Cr moments, rather than by spin canting. Therefore, we consider the collinear solution as the most likely ground state of the systems considered. This analysis is consistent
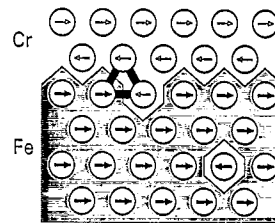

Fig. 10. Schematic picture of moments near a non-ideal Fe/Cr interface, with a Cr interface impurity and with a Cr impurity atom within the Fe layer. The competing AF interactions between the atoms forming the triangle suppress the moment of the Cr interface impurity. The moment of the Cr impurity atom within the Fe layer is much higher.

with the observation from our calculations that for V-based systems, which show only a very weak V–V exchange interaction, V interface impurities have much larger induced moments.

5.2. Spin-dependent scattering

In an earlier paper [11] we have proposed a simple model which relates trends in the spin dependence of scattering at non-ideal interfaces to the magnetic moments of atoms in mixed interface layers. It starts with the point of view that diffusive scattering at non-ideal interfaces is the result of the lateral variation of the atomic scattering potential in the mixed interface layers. Following Itoh et al. [10] we relate the spin-dependent scattering potential, ΔV^{σ}, to the energy difference between the centers of mass of the spin-resolved 3d local densities of states of the two types of atoms, A and B, in the mixed layer. In the case of weak scattering, the first Born approximation may be applied. The spin dependent scattering probability is then proportional to $[\Delta V^{\sigma}]^2$, as well as to the density of states at the Fermi level [29]. In the following discussion on spin dependent scattering at non-ideal Fe/Cr and Fe/V interfaces we will focus on trends in the scattering potential, and neglect possible effects due to density of states variations.

We next assume that the energy difference between the d-band centers of mass is proportional to the difference between the numbers of occupied d-states (per atom) for the A and B atoms in the
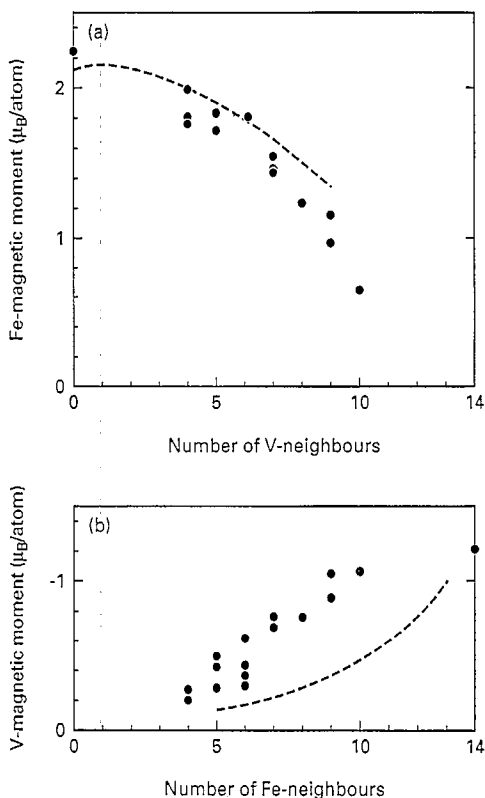

Fig. 9. Dependence of the calculated (a) Fe and (b) V magnetic moments, at perfect interfaces and in mixed interface layers of Fe/V superlattices (filled circles). The figure also includes the calculated bulk Fe moment and impurity V moment. The dashed lines give the average Fe and V moments for random substitutional bcc-type alloys, as a function of the average numbers of nearest neighbours, as calculated by Johnson et al. [27].

mixed interfacial planes. The scattering potential may therefore be expressed as:

$$\Delta V^{\sigma} = \Delta n_{d}^{\sigma}(A/B) \equiv n_{d}^{\sigma}(B,\text{int.}) - n_{d}^{\sigma}(A,\text{int.})$$

(1)

The approximation made is that the local d-density of states for both atoms have similar widths, and rectangular shapes. These assumptions are rather crude. However, it was shown in [11] that this approach may be used successfully to describe trends in the spin-resolved residual resistivity of dilute Fe–TM alloys (TM = 3d transition metal), using occupation number differences which were obtained from ASW band structure calculations.

The relationship between spin-dependent scattering and interface magnetism may be made after recognizing that in transition metal alloys atoms are (often within 0.1 electron) charge neutral, and that (within a few hundreds of μ_{B}) their magnetic moment results from the 3d-band polarisation, m. The occupation number difference may then be written as

$$\Delta n_{d}^{\sigma}(A/B) \simeq \mp \tfrac{1}{2}(m_{A} - m_{B}) - \tfrac{1}{2}(Z_{A} - Z_{B}),$$ (2)

where the − (+) sign refers to minority (majority) spin electrons, and where Z is the atomic number.

Eq. (2) implies that, in order to have minimal scattering of minority spin electrons, the moment differences $(m_{Fe} - m_{Cr,V})$ within the mixed layers should be equal to 2 and 3 μ_{B}, respectively. As shown in Fig. 4, this criterium is closely met for Fe/Cr systems: independent of the specific structure of the interface layer the difference between the Fe and Cr moments falls in the range 2.1–2.5 μ_{B}. This situation, with $\Delta n_{d}^{\downarrow}(Fe/Cr) = 0.05$–0.25, represents the case of very weak scattering, as may be seen from the similar discussion of impurity scattering [11]. The scattering potential for majority spin electrons is at least an order of magnitude larger. However, for Fe/V systems, the minority spin scattering potential is very small only for V interface impurities, whose induced moment of about −1 μ_{B} is about 3 μ_{B} lower than that of the Fe atoms in the interface layer. In mixed layers with higher V concentrations the average moment difference decreases, and reaches values of about 1.5 and 1.0 μ_{B} for (100) and (110) systems, respectively, in the limit of Fe interface impurities. Even in the most ideal MBE grown Fe/V superlattices, the entire range of local

interface concentrations is expected to be represented. Therefore, the minority spin interface scattering is expected to be significantly stronger than in the case of Fe/Cr. The fact that only very small GMR ratios for Fe/V systems have been obtained so far (highest observed value equals 6% at 4.2 K for (30 Å Fe/16 Å V) multilayers [30]) is consistent with this result. The analysis given above shows that the small Cr moments in the mixed interface layers are crucial to the small minority spin scattering at Fe/Cr interfaces.

Finally, we would like to compare scattering at mixed interface layers with scattering in bulk alloys. In contrast to scattering at non-ideal interfaces, the spin dependence of scattering in dilute Fe-based alloys is larger at V impurities than at Cr impurities [31,32], due to much smaller scattering of minority spin electrons in dilute FeV. Using the same approach to scattering as discussed above, we have shown in [11] that this may be understood as follows. The calculated impurity moments are −1.24 and −1.71 μ_{B}, respectively, leading to $\Delta n_{d}^{\downarrow}(FeCr) = +0.99$ and $\Delta n_{d}^{\downarrow}(FeV) = +0.25$, using the calculated bulk moment of 2.26 μ_{B} for bcc Fe. This implies that the minority spin scattering at Cr impurities is much stronger than at V impurities, due to the combined effect of the atomic number difference and the larger induced Cr moment. This picture is supported by very recent results by Butler et al. [26]. Their calculation of the concentration dependence of atom resolved moments and the spin resolved resistivity of random Fe–Cr alloys confirms that the relatively high minority spin residual resistivity is related to the high impurity moment, and that the contribution to the resistivity per atom decreases rapidly if, at higher Cr concentrations, the Cr moments become smaller.

5.3. Thermal stability of interfacial magnetism

The GMR ratio of Fe/Cr systems shows a very large decrease with temperature, typically a factor 5–6 from 4.2 K to room temperature for systems with at 4.2 K a GMR ratio above 100% [33–35]. In contrast, Co based systems show a much smaller decrease, less than a factor 2 for Co/Cu systems. An important contribution to the decrease with temperature of the GMR ratio is electron–magnon scattering,

which shortens the mean free path, and introduces spin mixing [35–37]. A measure of the spin wave softness is given by the parameter B, which follows from a fit to the temperature dependence of the magnetization far below the Curie temperature using the expression $M(T)/M(0) = 1 - BT^{3/2}$. Such a Bloch law $T^{3/2}$ expression is also valid for thin films, provided the magnetic layers are sufficiently thick. However, the parameters B are different for the magnetization in the bulk of a magnetic layer, and at the interface. For bulk Co, B is more than a factor 2 smaller than for bulk Fe. This may explain part of the different temperature dependences of the GMR ratio for Co/Cu and Fe/Cr systems. In the following we consider the additional effect of electron–magnon scattering at the interfaces.

Our investigation of interfacial magnetism of non-ideal Fe/Cr interfaces, has revealed that competing exchange interactions result in frustration and therefore, at $T = 0$, in a relatively shallow energy minimum. As a consequence, magnons at non-ideal Fe/Cr interfaces are expected to be relatively soft, and electron magnon scattering is expected to be much larger at the interfaces, than in the bulk of the layers. This suggestion is, qualitatively, consistent with the observation for Fe/Cr systems by Gijs et al. that in the CPP geometry, which favours transport through interfaces, the temperature dependence of the GMR ratio is much larger than in the CIP geometry [35].

In order to discuss this point more quantitatively, we first note that the interface value of B has been discussed theoretically by Rado [38] and by Mills and Maradudin [39]. The latter authors studied the case of thick magnetic layers between thick nonmagnetic layers, treating Fe–Fe exchange within the Heisenberg model. Within this model, the ratio $\alpha_{int} \equiv B_{int}/B_{bulk}$ is predicted to be equal to 2, in agreement with the earlier prediction by Rado based on a continuum model of a smooth interface. Experimental studies of layer-resolved spin wave parameters, using [57]Fe Mössbauer spectroscopy, have revealed close agreement with theory for the close-packed Fe(110)/Ag(111) interfaces, for which $\alpha_{int} = 2.3$ [40] and $\alpha_{int} = 1.86$ [41] have been obtained. The additional Cr–Cr and Fe–Cr interactions complicate the situation for Fe/Cr interfaces. In the case of non-ideal interfaces, one would expect that the com-

peting exchange interactions may result in a α_{int} parameter considerably exceeding 2, its precise value depending on the detailed type of interface roughness. Mössbauer studies by Landes et al. [42] have indeed revealed such an effect, viz. $\alpha_{int} = 3.3$ for a comparatively rough Fe/Cr(110) interface. On the other hand, experiments by Zukrowski et al. [43] have shown that in the case of smooth Fe/Cr(110) interfaces B_{int} is enhanced by a factor smaller than 2. In the latter case, the magnetism of Cr apparently stabilizes interfacial magnetism.

In agreement with our theoretical discussion, interfacial roughness thus has a strong effect on the thermal stability of interfacial magnetism. It would be of much interest (i) to extend the Mössbauer studies to the case of Fe/Cr(100), and (ii) to model the temperature dependence of the CPP GMR effect of microstructured Fe/Cr systems, in order to quantitatively disentangle bulk and interfacial contributions to electron–magnon scattering.

6. Summary

In this paper, the first systematic study has been presented of the magnetic moments at non-ideal Fe/Cr and Fe/V interfaces. For Fe/V superlattices magnetic moments in mixed monolayers at the interfaces are found to be strongly related to their local environment. As in random substitutional bulk alloys, Fe and V moments decrease (increase) with an increasing number of V (Fe) neighbours. However, for a given number of Fe nearest neighbours, V moments at interfaces are significantly larger than V moments in random alloys. This may be explained on the basis of the larger average magnetic moments of the Fe neighbours in the case of V atoms at an interface. Fe and Cr moments at Fe/Cr interfaces show no significant dependence on the environment. Cr moments in mixed interface layers have low magnetic moments, even when they have as many as 10 Fe neighbour atoms. We have explained this remarkable phenomenon as the result of competing antiferromagnetic Fe–Cr and Cr–Cr exchange interactions. Using a simple model for trends in electron scattering at non-ideal interfaces, we argued that the strong spin-dependence of scattering at non-ideal Fe–Cr interfaces is the result of the suppression of

Cr magnetism due to the frustration effect mentioned above. This picture explains why for Fe/Cr superlattices only in the case of a moderate degree of imperfectness of the interfaces (roughness, but no interdiffusion) a high GMR ratios is obtained.

Acknowledgements

References

[1] B. Dieny, J. Phys.: Cond. Matter 4 (1992) 8009.
[2] B.A. Gurney, V.S. Speriosu, J.-P. Nozières, H. Lefakis, D.R. Wilhoit and O.U. Need, Phys. Rev. Lett. 71 (1993) 4023.
[3] M.A.M. Gijs and M. Okada, Phys. Rev. B 46 (1992) 2908; S.K.J. Lenczowski, M.A.M. Gijs, J.B. Giesbers, R.J.M. van de Veerdonk and W.J.M. de Jonge, Phys. Rev. B 50 (1994) 9982; S.K.J. Lenczowski, M.A.M. Gijs, R.J.M. van de Veerdonk, J.B. Giesbers and W.J.M. de Jonge, MRS Symp. Proc. Spring Meeting 1995 (to be published).
[4] W.P. Pratt, Jr., S.-F. Lee, J.M. Slaughter, R. Loloee, P.A. Schroeder and J. Bass, Phys. Rev. Lett. 66 (1991) 3060; Q. Yang, P. Holody, R. Loloee, L.L. Henry, W.P. Pratt, Jr., P.A. Schroeder and J. Bass, Phys. Rev. B 51 (1995) 3226 (and references therein).
[5] S.S.P. Parkin, Phys. Rev. Lett. 71 (1993) 1641.
[6] R. Schad, C.D. Potter, P. Beliën, G. Verbanck, V.V. Moschalkov and Y. Bruynseraede, Appl. Phys. Lett. 64 (1994) 3500.
[7] S.T. Purcell et al., Phys. Rev. Lett. 67 (1991) 903; J. Unguris, R.J. Celotta and D.T. Pierce, Phys. Rev. Lett. 67 (1991) 140; S. Democritov, J.A. Wolf, P. Grünberg and W. Zinn, Mater. Res. Soc. Symp. Proc. 231 (1992) 133.
[8] S. Handschuh, PhD thesis, University of Köln (1994).
[9] P. Beliën, R. Schad, C.D. Potter, G. Verbanck, V.V. Moschalkov and Y. Bruynseraede, Phys. Rev. B 50 (1994) 9957; R. Schad, C.D. Potter, P. Beliën, G. Verbanck, J. Dekoster, G. Langouche, V.V. Moshchalkov and Y. Bruynseraede, J. Magn. Magn. Mater. 148 (1995) 331.
[10] H. Itoh, J. Inoue and S. Maekawa, Phys. Rev. B 47 (1993) 5809.
[11] R. Coehoorn, J. Magn. Magn. Mater. 121 (1993) 432.
[12] K. Adachi, in: Landolt-Börnstein, New Series III/19a (Springer, Berlin, 1986) p. 352.
[13] H. Dreyssé, A. Vega, D. Stoeffler, J. Khalifeh and C. Demangeat (preprint).
[14] R. Coehoorn, in: Proceedings of the 14th International Colloquium on Magnetic Films and Surfaces, Düsseldorf (1994), p. 608.
[15] A.R. Williams, J. Kübler, C.D. Gelatt, Jr. Phys. Rev. B 19 (1979) 6094.
[16] U. von Barth and L. Hedin, J. Phys. C 5 (1972) 1629.
[17] J.F. Janak, Sol. State Comm. 25 (1978) 53.
[18] Y. Wang, P.M. Levy and J.L. Fry, Phys. Rev. Lett. 65 (1990) 2732.
[19] F. Herman, J. Sticht and M. van Schilfgaarde, J. Appl. Phys. 69 (1991) 4783.
[20] N. Hamada, K. Terakura and A. Yanase, J. Magn. Magn. Mater. 35 (1983) 7.
[21] A. Vega et al., J. Appl. Phys. 69 (1991) 4544.
[22] D. Stoeffler and F. Gautier, Progress of Theoretical Physics 101 (1990) 139.
[23] T. Shinjo, Surf. Science Reports 12 (1991) 49.
[24] R. Coehoorn, J. Magn. Magn. Mater. (1995), to be published.
[25] P. Koorevaar, Y. Suzuki, R. Coehoorn and J. Aarts, Phys. Rev. B 49 (1994) 441.
[26] W.H. Butler, X.-G. Zhang, D.M. Nicholson and J.M. MacLaren, J. Magn. Magn. Mater. 151 (1995) 354 (this issue).
[27] D.D. Johnson, F.J. Pinski and J.B. Staunton, J. Appl. Phys. 61 (1987) 3715.
[28] D. Stoeffler and F. Gautier, in: Magnetism and Structure in Systems of Reduced Dimension, eds. R.C. Farrow et al. (Plenum, New York, 1993).
[29] J.S. Dugdale, in: The Electrical Properties of Metals and Alloys (Edward Arnold, London, 1977) p. 120.
[30] Y. Suzuki and R. Coehoorn (unpublished).
[31] J.W.F. Dorleijn and A.R. Miedema, J. Phys. F 5 (1975) 487.
[32] I.A. Campbell and A. Fert, in Ferromagnetic Materials, vol.3, ed. E.P. Wohlfarth (North-Holland, Amsterdam, 1982) p.747.
[33] W. Folkerts, W. Hoving and W. Coene, J. Appl. Phys. 71 (1992) 362.
[34] E.E. Fullerton, M.J. Conover, J.E. Mattson, C.H. Sowers and S.D. Bader, Phys. Rev. B 48 (1993) 15755.
[35] M.A.M. Gijs, S.K.J. Lenczowski and J.B. Giesbers, Phys. Rev. Lett. 70 (1993) 3343.
[36] J.E. Mattson, M.E. Brubaker, C.H. Sowers, M. Conover, Z. Qui and S.D. Bader, Phys. Rev. B 44 (1991) 9378.
[37] P. Bruno and A. Fert, in: Ultrathin Magnetic Structures, vol. 2, eds. J.A.C. Bland and B. Heinrich (Springer, Berlin, 1994).
[38] G.T. Rado, Bull. Am. Phys. Soc. 112 (1957) 127.
[39] D.L. Mills and A.A. Maradudin, J. Phys. Chem. Solids 28 (1967) 1855.
[40] J. Korecki and U. Gradmann, Europhys. Lett. 2 (1986) 651.
[41] D.J. Keavney, D.F. Storm, J.W. Freeland, M.D. Wieczorek, J.C. Walker, M.G. Pini, P. Politi and A. Rettori, Phys. Rev. Lett. 71 (1993) 927.
[42] J. Landes, C. Sauer, S. Dörrer and W. Zinn, J. Magn. Magn. Mater. 113 (1992) 137.
[43] J. Zukrowski, G. Liu and U. Gradmann, J. Magn. Magn. Mater. 140–144 (1995) 1977.